Research Article
Study of the Photothermal Response of a Monofacial Solar Cell in Dynamic Regime Under a Multispectral Illumination

[1]N. Thiam, [1]A. Diao, [2]M. Wade, [1]M. Ndiaye, [3]I. Zerbo, [4]M. Sarr, [5]A. S. Maïga and [1]G. Sissoko
[1]Laboratory of Semiconductors and Solar Energy, Physics Department, Faculty of Science and Technology, University Cheikh Anta Diop, Dakar, Senegal
[2]Ecole Polytechnique of Thies, EPT, Thies, Senegal
[3]Laboratory of Materials and Environment, UFR/SEA, University of Ouagadougou, Burkina Faso
[4]University of Thies, UFR SET, Thies, Senegal
[5]Section of Applied Physics, UFR SAT, Gaston Berger University, Dakar

Abstract: In this study, we present the study of the photo-thermal response of a monofacial silicon solar cell illuminated by a multispectral light for a constant modulated frequency. Solving the continuity equation for minority carriers in the base of the solar cell resulting in the terms of the heat equations in the presence of an optical source. The density of minority carriers in excess, the amplitude of the variation of temperature and the heat flux density were studied and analyzed for different angular pulses and rates of recombination at the junction. Representations of Nyquist and Bode plots of the thermal dynamic impedance resulted in an equivalent electrical circuit of the photocell.

Keywords: Capacitive effect, inductive effect, photothermal, pulse, solar cell

INTRODUCTION

The efficiency of a solar cell depends among others on its intrinsic parameters. Therefore the knowledge of these parameters and control of associated technological processes highlighted below are essential for any improvement of the conversion efficiency expected from the solar cell. Various characterization techniques have been implemented both in static frequency regime (Barro *et al*., 2001; Lemrabott *et al*., 2008) and in dynamic i.e transient regime (Dieng *et al*., 2007; Barro *et al*., 2003)

In this study we are aiming at studying the influence of the multispectral pulse and the recombination velocity at the interface (S_f) on the density of minority carriers in excess due to the variation in temperature and the density of heat flow. Through the operating performances of Nyquist and Bode plots for the thermal impedance, we established an equivalent electrical circuit of the photocell.

THEORY

Photovoltaic response (minority carrier density in excess): We consider solar silicon with a Back Surface Field (B.S.F) for the structure n^+-p-p^+ (Le Quang Nam *et al*., 1992).

Given that the contribution of the base to the photocurrent is larger than that of the emitter (Barro *et al*., 2001; Lemrabott *et al*., 2008), the univariate analysis will only be developed in the base region. In addition, we consider the hypothesis of Quasi-Neutral Base (Q.N.B) neglecting the crystal field within the solar cell.

In Fig. 1 we present a schematic sketch of a multicrystalline silicon solar cell with a Back Field (BSF) typically n^+- p - p^+.

The solar cell is subjected to a constant multispectral illumination from a source of a modulated frequency and the phenomena of generation, diffusion and recombination of photogenerated carriers in the base are considered. These phenomena are governed by the continuity equation:

$$D(\omega).\frac{\partial^2\delta(x,t,\omega)}{\partial x^2}-\frac{\delta(x,t,\omega)}{\tau}+G(x,t)=\frac{\partial\delta(x,t,\omega)}{\partial t} \quad (1)$$

For a given frequency, the terms d(x, t) and G (x, t) represent respectively the carrier density and the rate of optical generation (Hollenhorst and Hasnain, 1995;

Corresponding Author: G. Sissoko, Laboratory of Semiconductors and Solar Energy, Physics Department, Faculty of Science and Technology, University Cheikh Anta Diop, Dakar, Senegal
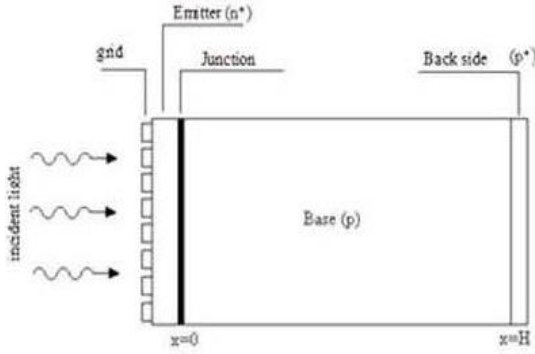
Fig. 1: A monofacial solar cell a multispectral illumination from a modulated frequency

Flohr and Helbig, 1989) and such above functions of time are expressed as follows:

$$\delta\,(x, t) = \delta(x).e^{i.\omega.t} \tag{2}$$

$$G(x, t) = g(x).e^{i.\omega.t} \tag{3}$$

d(x) et g(x) are standing for spatial components of the carrier density and the rate of generation.

The term $e^{i.\omega.t}$ represents the time component for the carrier density and the rate of optical generation. Comparing the above equations for which incident optical beam and the density of photogenerated carriers, the Eq. (1) is simplified and becomes as follows:

$$\frac{\partial^2\delta(x)}{\partial x^2} - \frac{\delta(x)}{L(\omega)^2} + \frac{g(x)}{D(\omega)} = 0 \tag{4}$$

The parameter $D(\omega)$ is given by the following expression (Neugroschel *et al.*, 1978):

$$D(\omega) = D.\left[\frac{1+\omega^2\tau^2}{(1-\omega^2\,\tau^2)^2+(2\omega\tau)^2} + i.\,\omega\tau\,\frac{-1-\omega^2\tau^2}{(1-\omega^2\,\tau^2)^2+(2\omega\tau)^2}\right] \tag{5}$$

and

$$\frac{1}{L(\omega)^2} = \frac{1}{Ln^2} \times (1 + i\,.\omega\tau) \tag{6}$$

where, $L(\omega)$ is the complex scattering length.

The spatial component g(x) is a rate of optical generation of electron-hole pairs for a multispectral illumination from a constant modulated frequency and as it reflects the entire spectrum of useful radiation incident on the solar cell, it is thus given by the following expression:

$$g(x) = \sum_{\lambda_0}^{\lambda_g} a(\lambda).\varnothing(\lambda)\,.\,[1 - R(\lambda)].e^{-a(\lambda).x} \tag{7}$$

where, $\alpha(\lambda)$ and $R(\lambda)$ represent respectively the absorption coefficient and the reflection coefficient of

the material for a given wavelength λ; φ(λ) is the flux of incident photons.

The extreme values of the wavelengths of the spectrum of solar radiation useful for the silicon are: $\lambda_0 = 0.3\mu m$ and $\lambda_g = 1.12\mu m$.

The density of minority charge carriers in excess (electrons), in fact and a solution of the Eq. (5):

$$\delta(x) = A_1(\omega).ch\left(\frac{x}{L(\omega)}\right) + A_2(\omega).sh\left(\frac{x}{L(\omega)}\right) +$$
$$\sum_{\lambda_0}^{\lambda_g} k(\omega,\lambda)\,.\,e^{-a(\lambda).x} \tag{8}$$

With

$$k(\omega, \lambda) = \frac{a(\lambda).\varnothing(\lambda).[1-R(\lambda)].L(\omega)^2}{D(\omega)^2.[1-L(\omega)^2.a(\lambda)^2]} \tag{9}$$

Using the boundary conditions (Dieng *et al.*, 2007) presented in Eq. (10) and (11), the coefficients $A_1(\omega)$ and $A_2(\omega)$ are determined.

At the emitter-base junction (x = 0) of the solar cell:

$$\frac{\partial\delta(x)}{\partial x}\,|_{x=0} = S_f\,.\,\frac{\delta(0)}{D(\omega)} \tag{10}$$

At the rear side of the cell base (x = H):

$$\frac{\partial\delta(x)}{\partial x}\,|_{x=H} = -\,S_b\,.\,\frac{\delta(H)}{D(\omega)} \tag{11}$$

S_f and S_b are respectively the recombination velocity at the junction and at the rear surface of the base.

The recombination velocity S_f is imposed by a varying impedance of an external load and by the interface states at the junction:

$$S^f = S_{f0} + S_{fm} \tag{12}$$

Indeed, S_f is the sum of two contributions:

S_{f0} is the intrinsic recombination velocity (depending only on the intrinsic parameters of the solar cell and is induced by the shunt resistor),

$S_{fm \text{ reflects the}}$ leakage current induced by the external load and for the operating point of the solar cell (Diallo *et al.*, 2008; Dème *et al.*, 2009).

Photothermal response (excess temperature across the solar cell): When a solar cell is subjected to a multi-spectral optical excitation from a constant modulated frequency, the minority charge carrier (electrons) is generated in the base. The movement of such carriers (diffusion and migration) in the solar cell generates a heat flux and an excessive temperature different from the equilibrium temperature of the material.

For a small temperature change compared to the initial temperature T_o, the heat flux in the solar cell can be described by the Eq. (13):

$$\alpha \cdot \frac{\partial^2 \Delta T(x,t)}{\partial x^2} + \frac{G_H(x,t)}{\rho.c} = \frac{\partial \Delta T(x,t)}{\partial t} \qquad (13)$$

The terms $\Delta T\,(x, t)$ and $G_H\,(x, t)$ which represent the change in temperature from the initial temperature T_o and the rate of heat generation with time written:

$$\Delta T(x,\,t) = \Delta T(x)e^{i.\omega.t} \qquad (14)$$

$$G_H(x,\,t) = G_H(x) \pm e^{i.\omega.t} \qquad (15)$$

$\Delta T(x)$ and $G_H(x)$ are the spatial components of the temperature and rate of heat generation.

The term $e^{i.\omega.t}$ represents the time component of the temperature and rate of heat generation. This time component has the same pulse $\omega = 2.\pi.f$ as the incident optical beam at each time t.

Equation (13) can be rewritten:

$$\frac{d^2 \Delta T(x)}{dx^2} - \sigma\,(\omega)^2 \cdot \Delta T(x) + \frac{G_H(x)}{k} = 0 \qquad (16)$$

With

k = a . ρ . c thermal conductivity of the material:

$$\sigma(\omega) = \left(\frac{i.\omega}{a}\right)^{1/2}$$

the complex thermal diffusion coefficient of the material.

The spatial component $G_H\,(x)$ the rate of heat generation is given by the equation:

$$G_H(x) = \sum_{\lambda_0}^{\lambda_g} a(\lambda).\emptyset(\lambda)\,.\,[1 - R(\lambda)].\,\Delta E(\lambda).e^{-a(\lambda).x}$$
$$+ \frac{E_g.\,\delta(x)}{\tau} \qquad (17)$$

where,

E_g is the energy gap of the semiconductor material $\Delta E = h.\upsilon - E_g$ is the energy thermalization resulting from the relaxation of optically excited carriers was due to absorption of photons of energy greater than the energy gap Eg.

The heat Eq. (13) can be expressed as:

$$\frac{d^2 \Delta T(x)}{dx^2} - \sigma\,(\omega)^2 \cdot \Delta T(x) + \frac{E_g}{k.\tau}\left\{A_1(\omega).ch\left(\frac{x}{L_\omega}\right) + \right.$$
$$A_2(\omega).sh\left(\frac{x}{L_\omega}\right)\Bigg\} - \sum_{\lambda_0}^{\lambda_g}\frac{a(\lambda).\emptyset(\lambda).[1-R(\lambda)]}{k}\Bigg\{\Delta E +$$
$$\frac{E_g.L(\omega)^2}{D(\omega).\tau.(1-\alpha^2.L_\omega^2)}\Bigg\}.e^{-a(\lambda).x} \qquad (18)$$

The excess temperature of the movement of minority carriers in the material, solution of the above equation is of the form:

$$\Delta T(x, \omega) = C_1(\omega).ch(\sigma.\,x) + C_2(\omega).sh(\sigma.\,x)$$
$$+ \frac{E_g}{k.\tau(\sigma^2 - L_\omega^{-2})}\left\{A_1(\omega).ch\left(\frac{x}{L_\omega}\right) + A_2(\omega).sh\left(\frac{x}{L_\omega}\right)\right\}$$
$$+ \sum_{\lambda_0}^{\lambda_g}\frac{a(\lambda).\emptyset(\lambda).[1-R(\lambda)]}{k.[\sigma(\omega)^2 - a(\lambda)^2]}\left\{\Delta E + \frac{E_g.L(\omega)^2}{D(\omega).\tau.[1-\alpha(\lambda)^2.L(\omega)^2]}\right\}.e^{-a(\lambda).x} \qquad (19)$$

The constants C_1 (w) and C_2 (w) are determined by the boundary conditions (20) et (21)

- At the emitter-base junction (x = 0)

$$\left.\frac{d\Delta T(x)}{dx}\right)_{x=0} = \frac{S_f.E_g}{k} \cdot \delta(0) \qquad (20)$$

- At the rear of the base (x = H)
$$\left.\frac{d\Delta T(x)}{dx}\right)_{x=H} = \frac{-S_b.E_g}{k} \cdot \delta(H) \qquad (21)$$

RESULTS

Photovoltaic response (profile of the density of minority carrier charge): Figure 2 and 3 show the profile curves of module density of charge carriers in the base of the solar cell, respectively, in a situation of short circuit and open circuit. These curves highlight the influence of the pulse angle.

For the model operating in short circuit as illustrated in Fig. 2 and for each pulse there is a position x_0 in the base where the gradient of the density of minority carriers is zero. Increasing the angular pulsation leads to an increase in the density of minority carriers in the base and a decrease of the value x_0. This is due to among others the relaxation (Ndiaye *et al.*, 2008). Considerable losses of the minority carrier density observed at deeper positions for a large frequency is due to bulk recombination (Ricaud, 1997). Such a recombination is less important for low frequencies i.e for high wavelengths.

For the case of open circuit, the minority carrier density decreases with the pulse angle. The curves show a zero gradient in the vicinity of the junction.

We observe an inversion pulse with the angular values for the relatively low pulse, 10^4 rad/s<w<10^5 rad/s.

In deeper positions in the base like for the short circuit model, the phenomena of recombination increase with the pulse angle; and for the depths of about 100 mm the density of minority carriers is almost zero.

Photothermal response (profile of the temperature variation):
Study according to the depth: Figure 4 and 5 show the evolution of temperature versus the base depth respectively for a solar cell operating in a situation of short circuit and in case of open circuit model. The influence of the excitation pulse is highlighted.
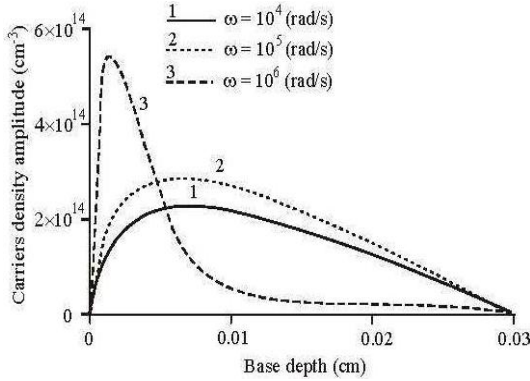
Fig. 2: Minority carrier density versus the depth for different values of the pulse. The case of short circuit, Sf_0: 10^3 cm/s; Sfm: 8.10^8 cm/s; H: 0.03μm: D: 26 cm²/s

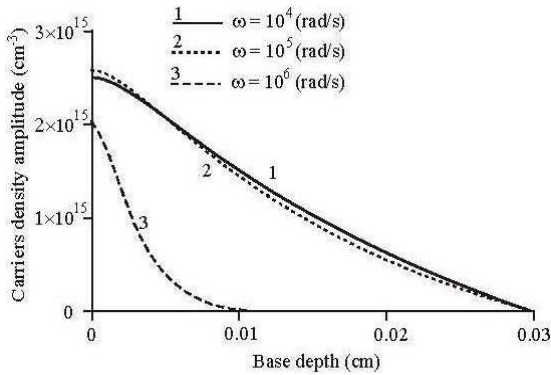Fig. 3: Minority carrier density as a function of the depth for different values of the pulse. The case of open circuit, Sf_0: 10^3 cm/s; S_{fm}: 8.10^8 cm/s; H: 0.03μm: D: 26 cm²/s
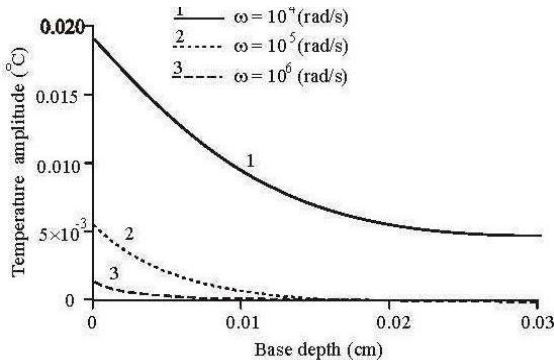
Fig. 4: Profile for the change in temperature versus the base depth for a solar cell in short circuit model, D: 26 cm²/s, H: 0.03 μm; a: 1 cm²/s; k: 1.54 W/cm. °C, S_{f0}: 10^3 cm/s, S_{fm}: 8.10^8 cm/s

For the situation in the short circuit, Fig. 4, the temperature amplitude is maximum at the junction of the solar cell and then decreases with depth in the base zone. Increasing the angular the signal pulse causes a decrease in the temperature amplitude within the solar
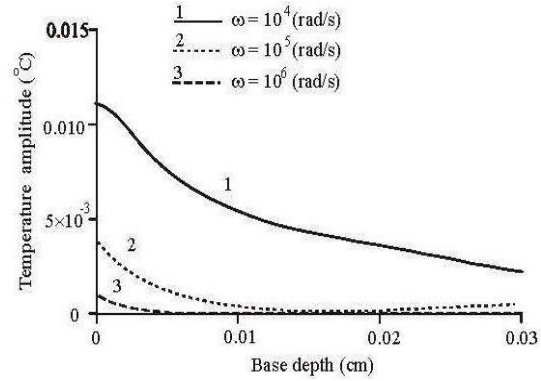

Fig. 5: Temperature as a function of depth in the base, open circuit, D: 26 cm²/s; H: 0.03 μm; a: 1 cm²/s; k: 1.54 W/cm. °C; S_{f0}: 10^3 cm/s, S_{fm}: 0 cm/s

cell bulk. Near the junction, the absorbed short wavelengths of the incident solar radiation spectrum result in significant generation of carriers at high values of energy (i.e. greater than the energy gap for a silicon material). These high energy excess of photogenerated carriers near the junction is lost due to the thermalization, a phenomenon justifying the high values of the excess temperature observed at the junction of the solar cell. In addition, the temperature is maximum at the junction in a position of short circuit since the junction is the focal point of the charge carriers photogenerated within the base of the solar cell. In fact, the presence of a large number of carriers in the base region near the junction results in a major source of heat flux and then in higher temperatures. Like the density of minority charge carriers, the temperature amplitude is strongly influenced by the pulse signal.

In fact, for pulses $\omega \leq \omega_c$ ($\omega_c = 10^4$ rad/s) the temperature variation is not influenced by the frequency of the pulse; this is a status of quasi-static regime. Instead, for pulses $\omega > \omega_c$ the temperature variation is strongly influenced by the pulse; it is regarding the case of a non-static frequency regime.

The temperature is decreasing when the base depth is increased for a given angular pulsation.

However, for a given depth of the base and a given angular pulse, the amplitude of temperature, in case of short circuit model, is greater than for the open circuit situation. In fact, in case of the model of open circuit the photogenerated charge carriers are blocked near the junction, the temperature rise is due to the phenomenon of thermalization of photogenerated carriers near the junction. In addition the junction is blocked; there are more dimensions of bearers at this level and therefore more of an impact at the junction than elsewhere in the base of the solar cell.

Profiles of temperature versus the pulse and the recombination velocity:
Profile of the temperature variation as a function of the pulse angle: We present in Fig. 6 the profile of the
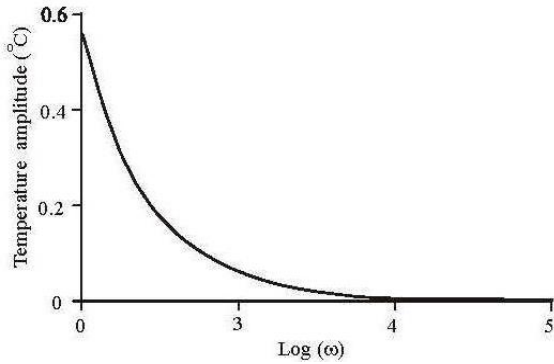
Fig. 6: Temperature variation versus the logarithm of the pulsation, D: 26 cm²/s; H: 0.03 μm; a: 1 cm²/s; k: 1.54 W/cm. °C; S_{f0}: 10^3 cm/s
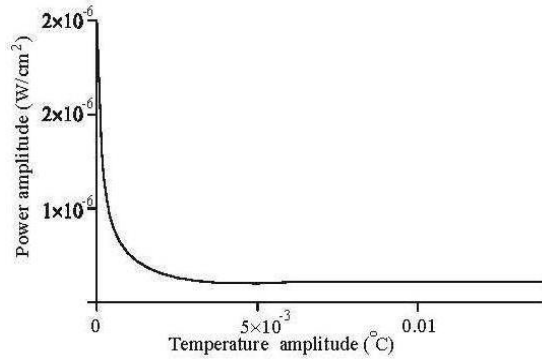

Fig. 8: Profile of power as a function of the temperature variation, D: 26 cm²/s; H: 0.03 μm; A: 1 cm²/s; k: 1.54 W/cm. °C; S_{f0}: 10^3 cm/s
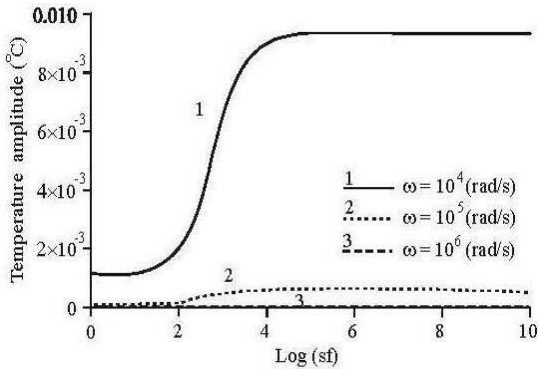

Fig. 7: Temperature variation depending on recombination tare at the junction for different values of the pulsation, D: 26 cm²/s; H: 0.03 μm; a: 1 cm²/s; k: 1.54 W/cm. °C; S_{f0}: 10^3 cm/s
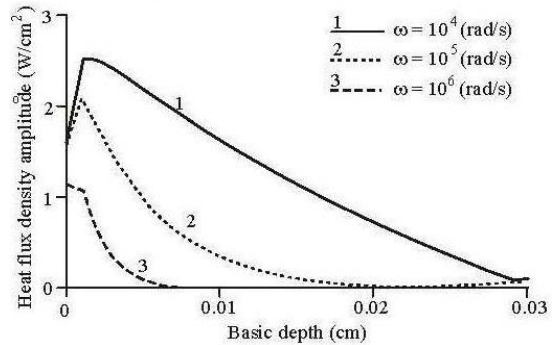

Fig. 9: Density of heat flux as a function of depth for different values of the pulsation in open circuit, D: 26 cm²/s; H: 0.03 μm; a: 1 cm²/s; k: 1.54 W/cm. °C; S_{f0}: 10^3 cm/s; S_{fm}: 8.10^8 cm/s

module temperature as a function of the pulse angle. The temperature at the junction of the solar cell is a decreasing function of the pulse angle modulation. Indeed the increase of the pulse causes a reduction in the density of photogenerated carriers which in return results in the decrease of temperature in the solar cell.

Profile of the temperature variation depending on the recombination velocity at the junction of the solar cell: We present in Fig. 7 the variations of temperature depending on the recombination velocity at the interface for different values of the depth x in the base.

According to the curves presented in Fig. 6, we observe that the temperature at the junction of the solar cell is an increasing function of recombination velocity at the junction for a given pulse. The temperature variation is less important for low values of recombination velocity at the interface (open circuit); it becomes high and the large asymptotic values of the recombination velocity at the junction (short circuit). This is in good agreement with results from the analysis

made in above paragraph for the distribution of the temperature versus the base depth of the solar cell.

Impact of temperature change on electrical power delivered by the base of the solar cell according: We present in Fig. 8 the electrical power depending on the temperature variation.

Increasing the temperature inside the solar cell results in a loss of electrical power. Indeed, the temperature increase is detrimental to proper functioning of the solar cell.

Heat flux density: The density of heat flux in the solar cell is given by the relation (20):

Behaviour of the heat flux density in the solar cell: Short circuit and open circuit: For different values of the pulse angle, we present in Fig. 9 and 10 variations of the heat flux as a function of depth in the base, respectively in case of short circuit and open circuit.

The curves in Fig. 9 show the existence of a zero gradient in the vicinity of the junction, at a position x_0 on the pulse angle. Beyond the position x_0, the density of eat flux decreases in depth of the base. Increasing the
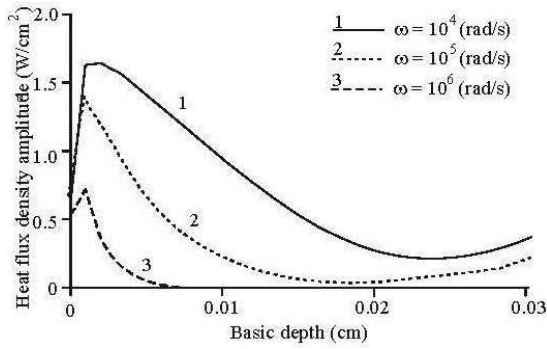
Fig. 10: Module of the density of heat flux as a function of depth for different values of the pulsation, D: 26 cm^2/s; H: 0.03 μm; a: 1 cm^2/s; k: 1.54 W/cm. ºC, S$_{f0}$: 10^3 cm/s; S$_{fm}$: 2.10^2 cm/s
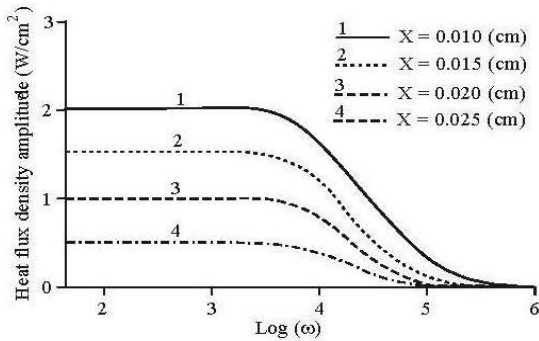

Fig. 11: Module of the heat flux density as a function the pulse angle for different values?? of the depth x (cm), D: 26 cm^2/s; H: 0.03 μm; a: 1 cm^2/s; K: 1.54 W/cm. ºC
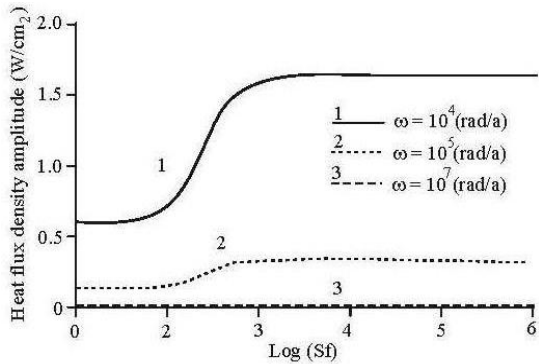

Fig. 12: Profile of the heat flus as a density as a function of rate recombination at the junction for different values??of pluse; D: 26 cm^2/s; H: 0.03 μm; a: 1 cm^2/s; k: 1.54 W/cm. ºC

angle of the signal pulse causes a decrease in the density of heat flow in the material. This is due to relaxation phenomena.

The behavior of charge carriers described in Fig. 4 and 5 is helpful and assists in understanding the distribution of the density of the heat flux.

Thus and in case of the open circuit situation, the charge carriers are blocked at the junction and the temperature rise is due to the phenomenon of thermalization of photogenerated carriers near the junction; with comparison to the situation of short circuit, the heat flux is higher for the open circuit.

Evolution as a function of angular pulsation: We present in Fig. 11 the profile of the heat flux density as a function of the logarithm of the pulse angle for different values of the depth x in the base.

The density of heat flow, for the different values of the pulse lower than 10^4 (rad/s), remains relatively constant; instead, the amounts of heat flux are smaller in case of higher frequencies; an inversion phenomenon is observed and occurs as described in Fig. 11 through a change in concavity of the curves for 10^4 rad/s<w<10^5 rad/s.

Evolution based on the recombination velocity at the junction of the solar cell: We present in Fig. 12 the profile of the density of heat flow based on the recombination velocity at the interface for different values of the depth x in the base.

For small values of the recombination velocity at the interface, the density of heat flow is low i.e the situation of open circuit. The flux density increases with larger values of recombination velocity at the interface and reaches its limit in case of short-circuit i.e. for S$_f$ higher than 10^4 cm/s. The heat flux density decreases when the angular pulsation is increasing.

Characteristic density of heat flow-temperature variation: We present in Fig. 13 the profile of the heat flux density as a function of temperature for different values of the depth x in the base.

The curves in Fig. 13 show the existence of an upper limit of the heat flux density when the temperature becomes important inside the solar cell. This is justified by a temperature gradient of zero, indicating a degree of uniformity of temperature within the base area.

The characteristic relationship between the temperature change and the density of heat flow proves that a dynamic behavior is linked to the role of impedance and to the analogy between electrical and thermal properties.

Thermal impedance of a solar cell: The dynamic thermal impedance (Ould Brahim *et al.*, 2011) for the solar cell is given by the following relation (21):

$$Z(\omega, x) = \frac{\Delta T(\omega, x)}{\emptyset(\omega, x)} \tag{21}$$

Nyquist representation of thermal dynamic impedance: Nyquist representation, Fig. 14, shows the evolution of the imaginary part of impedance as a function of its real part.
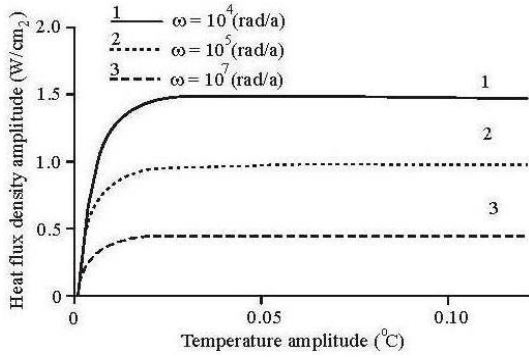
Fig.13: Heat flux density versus the amplitude of temperature, D : 26 cm^2/s ; H : 0.03 μm ; a : 1 cm^2/s ; k : 1.54 W/cm. °C
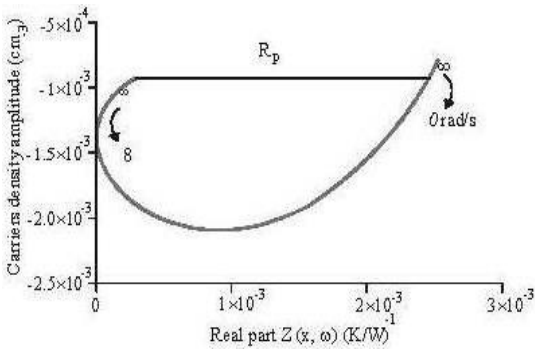
Fig. 14: Imaginary part according to the real part of impedance Z1, D: 26 cm^2/s; H: 0.03 μm
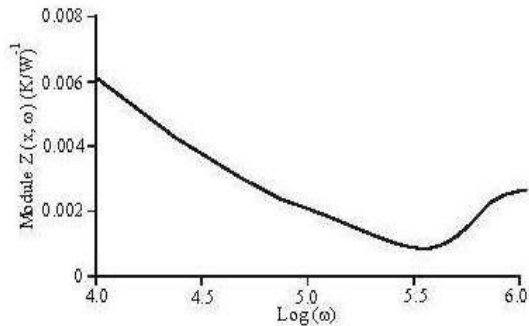
Fig. 15: Profile of the thermal impedance versus the logarithm of the pulsation, D: 26 cm^2/s; H: 0.03μm

Referring to the analogy established between the electrical and thermal behaviors, the imaginary part of the thermal impedance is negative and capacitance effects associated to the process of heat transfer in solar cell are significant.

Bode diagram of the dynamic impedance of the thermal solar cell: Through the Bode diagram of the impedance, the evolution of the phase of the impedance as a function of logarithm of the pulsation is presented in Fig. 15.
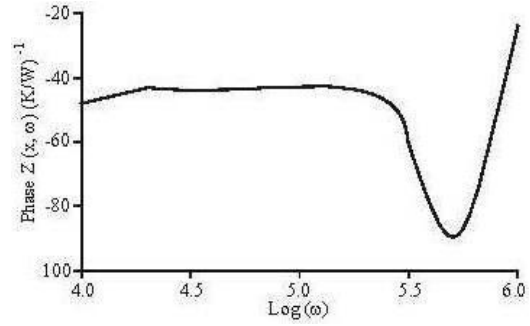

Fig. 16: Phase of the thermal impedance as a function the logarithm of the pulsation, D: 26 cm^2/s; H: 0.03 μm
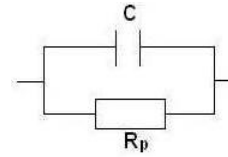

Fig. 17: Equivalent circuit of the solar cell

Figure 15 shows that the thermal impedance within the inversion region previously defined, i.e., 10^4 rad/s<w<10^5 rad/s, is decreasing when the pulse is increased. In fact any increase in the pulse results in a reduction for the density of minority carriers and in a decrease of temperature.

Bode diagram of the phase of dynamic thermal impedance: Within the pulse range of 10^4 rad/s<w<10^5 rad/s, the impedance phase is almost constant such an interval is representing the previously observed phenomenon of inversion. The phase of the impedance remains negative in such an inversion region considered above; the capacitive effects outweigh and dominate the inductive effects.

Equivalent circuit model of the dynamic impedance of the thermal solar cell: The thermal behaviour of the solar cell can be formulated as follows in Fig. 16. The capacitive effects and the variation of heat in the solar cell are linked; the resistance Rp reflects the heat transfer in the solar cell material.

The symbol C stands for the capacitance and Rp is an equivalent parallel and thus a diameter of the semicircle obtained in the representation of Nyquis (Dieng *et al*., 2011; Ly *et al*., 2011) (Fig. 17).

CONCLUSION

The formalism proposed in this study considered a solar cell operating under a multispectral illumination with a modulated frequency. Through the use of phenomenological parameters such as recombination velocities at the junction and the back of the base and the thermal behaviour of the solar cell, we analysed and

studied the density of minority charge carriers, the temperature amplitude and the density of heat flow. We found out that any increase in temperature results in a decrease of electrical power delivered by the base of the solar cell. For values of $\omega < 10^4$ rad/s, the density of minority carriers in excess, the variation of temperature and the heat flux density remain almost constant; such parameters are weakly influenced by the angle of the signal pulse: it is thus a situation of a static regime.

For values of $\omega > 10^4$ rad/s, the density of minority carriers in excess, the variation of temperature and the heat flux density decrease when the pulse angle of the signal increases: it is regarding a case of purely frequency regime and these parameters are highly dependent on the pulse angle.

Finally, the Nyquist and Bode diagrams of the impedance of the thermal dynamics for the solar cell have been helpful in establishing an equivalent electrical model for a solar cell under multispectral illumination.

NOMENCLATURE

D (ω) (cm^2/s) Diffusion $\varphi(\lambda)$ (cm^{-2}/s)Incident photon coefficient complex of flux the charge carriers λ_g (μm) The wavelength of ω (rad/s) Pulse angle of cutting of silicon estimated incident beam 1.12 μm L (ω) Diffusion length λ_0 (μm) The wavelength of complex carrier minority minimum the light source α (λ) (cm^1) Absorption (0.3 μm) coefficient of silicon H (cm) Thickness of the bace R (λ) Reflection of the solar cell coefficient of silicon T$_o$ (^{0}C) Initial temperature of at the wavelength λ the solar cell a (cm^2/s) Thermal ΔT (^{0}C) Temperature variation diffusivity of silicon σ (ω) Diffusion coefficient ρ (g/dm^3) Volume complex thermal silicon density of silicon E$_g$ (eV) Energy gap of silicon C (J/g^{0}C) Specific heat Φ (W/cm) Density of heat flow of siliconZ (^{0}C/W) Dynamic impedance k (W/cm^{0}C) Thermal thermal conductivity of silicon

REFERENCES

Barro, F.I., E. Nanema, A. Wereme, F. Zougmore and G. Sissoko, 2001. Recombination parameters measurement in silicon double sided surface field solar cell. J. Des. Sci., 1(1): 76-80.

Barro, F.I., E. Nanema, F. Zougmore, A. Wereme, A. Ndiaye and G. Sissoko, 2003. Transient study of double sided silicon solar cell under constant white bias light: Determination of recombination parameters. J. Des. Sci., 3(1): 10-14.

Dème, M.M., S. Sarr, R. Sam, S. Gueye, M.L. Samb, F.I. Barro and G. Sissoko, 2009. Influence of grain size, the recombination velocity at grain boundaries and the angle of incidence of light on the enlargement of the space charge zone of a solar cell monofaciale. J. Sci., 9(2): 17-27.

Diallo, H.L., A.S. Maiga, A. Wereme and G. Sissoko, 2008. New approach of both junction and back surface recombination velocities in a 3 D modeling study of a polycrystalline silicon solar cell. Europ. Phys. J. Appl. Phys., 42: 203-211.

Dieng, A., O.H. Lemrabott, A.S. Maiga, A. Diao and G. Sissoko, 2007. Impedance spectroscopy method applied to electrical parameters determination on bifacial silicon solar cell under magnetic field. J. of Sci., 7(3): 48-52.

Dieng, A., N. Thiam, A. Thiam, A.S. Maiga and G. Sissoko, 2011.Magnetic field effect on the electrical parameters of a polycrystalline silicon solar cell. Res. J. Appl. Sci. Eng. Techn., 3(7): 602-611.

Flohr, T. and R. Helbig, 1989. Determination of minority-carrier lifetime and surface recombination velocity by optical-beam-induced-current measurements at different light wavelengths. J. Appl. Phys., 66(7): 3060-3065.

Le Quang Nam, R.M., J. Nijs, M. Ghannam and J. Coppye, 1992. Spectral response of solar cells of high efficiency multicrystalline silicon. J. Phys. III, 2(7): 1305-1316.

Lemrabott, O.H., I. Ly, A.S. Maiga, A. Wereme, F.I. Barro and G. Sissoko, 2008. Bulk and surface recombination parameters measurement in silicon double sided solar cell under constant monochromatic illumination. J. Sci., 8(1): 44-50.

Hollenhorst, J.N. and G. Hasnain, 1995. Frequency dependent hole diffusion in InGaAs double heterostructures. Appl. Phys. Lett., 67(15): 2203-2205.

Ly, I., I. Zerbo, M. Wade, M. Ndiaye, A. Dieng, A. Diao, N. Thiam, A. Thiam, M.M. Dione, F.I. Barro, A.S. Maiga and G. Sissoko, 2011. Bifacial silicon solar cell under frequency modulation and monochromatic illumination: Recombination velocities and associated equivalent electrical circuits. Proceedings of the 26th European Photovoltaic Solar Energy Conference and Exhibition, Hamburg-Germany.

Neugroschel, A., P.J. Chen, S.C. Pao and F.A. Lindholm, 1978. Proc.13th Photovol. Sp. Conf. 70.

Ndiaye, M., Z.N. Bako, I. Zerbo, A. Dieng, F.I. Barro and G. Sissoko, 2008. Determination of electrical parameters of a solar cell under monochromatic frequency modulation, using diagrams Bode and Nyquist. J. Sci., 8(3): 59-68.

Ould Brahim, M.S., I. Diagne, S. Tamba, F. Niang and G. Sissoko, 2011. Characterization of the minimum effective layer of thermal insulation material two-plaster from the method of thermal impedance. Res. J. Appl. Sci. Eng. Techn., 3(4): 338-344.

Ricaud, A., 1997. Solar cells. Polytechnic and university presses romandes.